



# pH-Sensitive Polycations for siRNA Delivery: Effect of Asymmetric Structures of Tertiary Amine Groups

Qinping Yang, Yanliang Dong, Xuanyu Wang, Zhihao Lin, Mingyu Yan, Weiwei Wang, Anjie Dong, Jianhua Zhang,\* Pingsheng Huang,\* and Changrong Wang\*

pH-sensitive polyelectrolytes provide enormous opportunity for siRNA delivery. Especially, their tertiary amine structures can not only bind genes but also act as pH-sensitive hydrophobic structure to control genes release. However, the influence of molecular structures on siRNA delivery still remains elusive, especially for the asymmetric alkyl substituents of the tertiary amine groups. Herein, a library of *N*-methyl-*N*-alkyl aminoethyl methacrylate monomers (MsAM) with asymmetric alkyl substituents on the tertiary amine group is synthesized and used to prepare a series of tri-block polycationic copolymers poly(aminoethyl methacrylate)-block-poly(*N*-methyl-*N*-alkyl aminoethyl methacrylate)-block-poly(ethylene glycol methacrylate) (PAMA-PMsMA-PEG). And the properties of these polycations and their self-assembled micelles are characterized, including molecular structure, proton buffering capacity, pH-sensitivity, size, and zeta potential. With the length increase of one alkyl substituent, the proton buffering capacity of both monomers and polycations is demonstrated to be narrowed down. The siRNA delivery efficiency and cytotoxicity of these micelles are also evaluated on HepG2 cells. In particular, poly(aminoethyl methacrylate)-block-poly(*N*-methyl-*N*-ethyl aminoethyl methacrylate)-block-poly(ethylene glycol methacrylate) (PAMA-PMEMA-PEG) elicited the best luciferase knockdown efficiency and low cytotoxicity. Besides, PAMA-PMEMA-PEG/siRRM2 also induced significant anti-tumor activity *in vitro*. These results indicated PAMA-PMEMA-PEG has potential for further use in the design of gene vehicles with the improved efficiency of siRNA delivery.

## 1. Introduction

Small interfering RNA (siRNA), non-coding RNAs of 20–25 bp in length, can specifically suppress expression of target genes,<sup>[1]</sup> which have shown great potentials for a great many diseases.<sup>[2,3]</sup> Recently, several nuclei acid drugs have been applied to clinical trials.<sup>[4]</sup> However, the degradability by nuclei acid enzyme and electronegativity had serious impacts on siRNA systematic and intracellular delivery.<sup>[5,6]</sup> Therefore, developing an efficient siRNA delivery vehicle is extremely urgent.

Traditionally, the siRNA vehicles can be divided into two categories: virus vectors and non-virus vectors. Although viral vectors own high transfect efficiency, they also exhibit significant limitations, such as immunogenicity, limited load capacity, confined cytotropism, and complex analytical and production processes.<sup>[7,8]</sup> More importantly, the safety of viral vectors still limits their clinical trials.<sup>[9,10]</sup> Non-viral vehicles, as the viral vehicles succedaneum, have the advantages of low immunogenicity, low toxicity, and low cost.<sup>[11–13]</sup> Among the non-viral vehicles, the polycations have become the outshining tactics for gene delivery due to their controlled

Q. P. Yang, Y. L. Dong, X. Y. Wang, Z. H. Lin, M. Y. Yan, Prof. A. J. Dong, Prof. J. H. Zhang  
Department of Polymer Science and Engineering  
School of Chemical Engineering and Technology  
Tianjin University  
Tianjin 300072, China  
E-mail: jhuazhang@tju.edu.cn

Prof. W. W. Wang, Dr. P. S. Huang  
Tianjin Key Laboratory of Biomaterial Research  
Institute of Biomedical Engineering  
Chinese Academy of Medical Sciences and Peking Union Medical College  
Tianjin 300192, China  
E-mail: sheng1989.2008@163.com

Dr. C. R. Wang  
School of Pharmacy  
Shandong New Drug Loading & Release Technology and Preparation Engineering Laboratory  
Binzhou Medical University  
Yantai 264003, China  
E-mail: WCR20142014@163.com

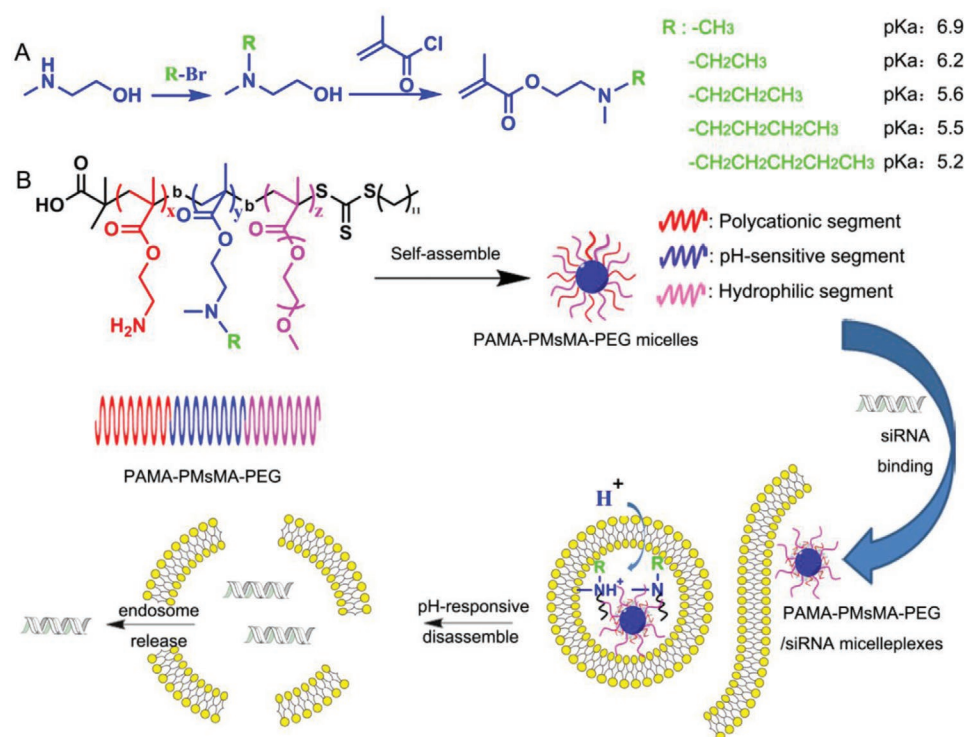
The ORCID identification number(s) for the author(s) of this article can be found under <https://doi.org/10.1002/mabi.202100025>.

DOI: 10.1002/mabi.202100025

preparation and flexible modification,<sup>[14]</sup> such as poly(2-dimethylaminoethyl methacrylate) (PDMAEMA),<sup>[15,16]</sup> polyethylenimine (PEI),<sup>[17]</sup> poly(L-lysine) (PLL),<sup>[18,19]</sup> and polyamidoamine dendrimer (PAMAM),<sup>[20]</sup> which could condense gene through charge interaction to form nanosized polyion complex (PIC). Such kind of vectors with abundant amine had presented excellent siRNA binding capacity and delivery efficiency, but the additional charge caused low biocompatibility and high biotoxicity. To evade the cytotoxicity induced by surplus charge, PEGylated strategies were generally brought to embellish polycations.<sup>[21,22]</sup> PEGylation polycations could improve biocompatibility, stability and prolong the circulation.<sup>[23]</sup> However, several shortcomings were introduced by PEGylation, named “PEG dilemma”, which not only hampered the interaction between siRNA and polycations but also inhibited the cell uptake and escape abilities.<sup>[24]</sup> In order to overcome the drawback of PEG dilemma, many approaches were adopted, such as integrating sheddable PEG<sup>[24,25]</sup> and introducing hydrophobization sections.<sup>[26]</sup> More importantly, the hydrophobization of polycations could not only resolve the PEG dilemma but also stabilize the PIC.<sup>[21,22,27]</sup> Particularly, the introduction of pH-sensitive sections into polycations to form pH-sensitive polycationic vehicles has drawn much attention, recently.<sup>[28]</sup> The pH-sensitive polycations are in favor of siRNA delivery, which is explained by “proton sponge effect”.<sup>[29,30]</sup> The amine groups of pH-sensitive section in polycations were protonated in acid endosome and induced the changes of osmotic pressure, resulting in the disruption of endosomal membrane and thus release of the cargo into cytosol.<sup>[31]</sup> Shen et al.<sup>[32–34]</sup> had analyzed the cancer gene-delivery cascade and the barriers, the needed nanoproperties.

Meanwhile, strategies such as stability, surface, and size transitions (3S Transitions) were proposed to resolve those dilemmas, which is to create efficient and low-toxicity nonviral gene vectors. However, The lower efficiency of cytosolic delivery of siRNA still is the bottleneck.<sup>[35,36]</sup>

In some previous studies, a library of polycationic micelles consisted of various hydrophobic sections with different pKa were evaluated on siRNA delivery,<sup>[37]</sup> and a significant discovery was that the pKa values of hydrophobic segments in the range of 5.8–6.2 induced higher siRNA delivery efficiency in vitro and in vivo.<sup>[38]</sup> These results indicated that the tertiary amine structures can not only bind genes but also act as pH-sensitive hydrophobic structure to exert significant influence on the siRNA delivery. However, the influence of molecular structures of the tertiary amine groups still remains remarkably elusive, especially for the asymmetric alkyl substituents. Herein, a new series of *N*-methyl-*N*-alkyl aminoethyl methacrylate monomers (MsMA, Alkyl = methyl, s = M; Alkyl = ethyl, s = E; Alkyl = propyl, s = P; Alkyl = butyl, s = B; and Alkyl = amyl, s = A), with asymmetric alkyl substituents on the tertiary amine groups, were synthesized and shown in **Scheme 1**. And the pH sensitivities of these monomers and the corresponding polymers were studied. The results reflected that the proton buffering capacity was narrowed down with the length increase of one alkyl chain. Furthermore, five tri-block polycations, poly(aminoethyl methacrylate)-block-poly(*N*-methyl-*N*-alkyl aminoethyl methacrylate)-block-poly(ethylene glycol methacrylate) (PAMA-PMsMA-PEG) were synthesized by reversible addition-fragmentation chain transfer (RAFT) polymerization. The physicochemical properties and



**Scheme 1.** Scheme diagrams of A) synthesis routes of pH-sensitive monomers with asymmetric *N*-alkyls substituents and B) formation of PAMA-PMsMA-PEG/siRNA micelleplexes with pH-responsive release of siRNA.

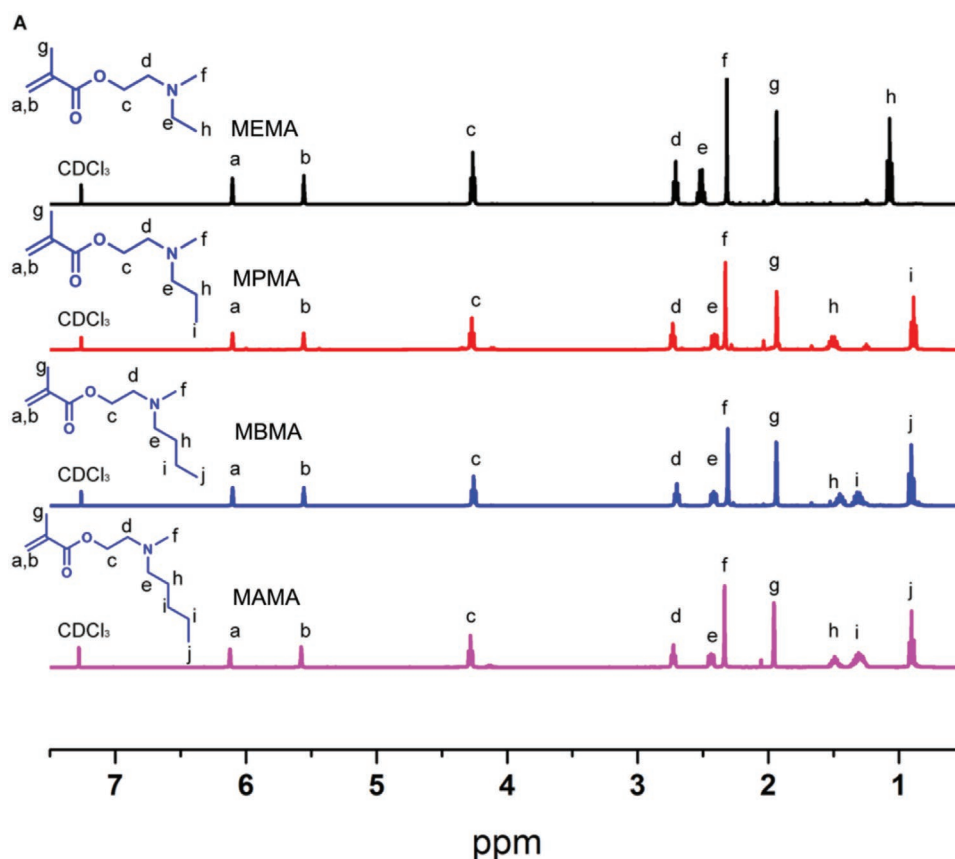


**Figure 1.** The  $^1\text{H}$  NMR spectra of MsMA monomers in  $\text{CDCl}_3$ .

bio-experiments of these polycations as siRNA vehicles in vitro were investigated. Compared with other polycations, poly(aminoethyl methacrylate)-block-poly(*N*-methyl-*N*-ethyl aminoethyl methacrylate)-block-poly(ethylene glycol methacrylate) (named as PAMA-PMEMA-PEG) with pKa values of 6.2 was found to possess higher gene knockdown efficiency, better biocompatibility, and higher anti-tumor efficiency in vitro, which can be used as an efficient siRNA delivery vehicles.

## 2. Results and Discussion

### 2.1. Synthesis and Characterizations of MsMA Monomers

A series of polymerizable and pH-sensitive monomers, *N*-methyl-*N*-alkyl aminoethyl methacrylate with asymmetric *N*-alkyls substituents, including *N*-methyl-*N*-ethyl aminoethyl methacrylate (MEAM), *N*-methyl-*N*-propyl aminoethyl methacrylate (MPAM), *N*-methyl-*N*-butyl aminoethyl methacrylate (MBAM), and *N*-methyl-*N*-amyl aminoethyl methacrylate (MAAM) were designed and synthesized by nucleophilic substitution and esterification reaction, as shown in Scheme 1A. Typically, *N*-methyl-*N*-alkyl ethanolamine was firstly synthesized by the nucleophilic substitution between *N*-methyl ethanolamine and corresponding 1-bromo alkane. And then the MsMA monomers were obtained by the reaction between

*N*-methyl-*N*-alkyl ethanolamine and methacryloyl chloride. The molecular structures of the obtained MsMA were characterized by  $^1\text{H}$  NMR, as shown in **Figure 1**. All  $^1\text{H}$  NMR spectra showed the characteristic peaks of carbon-carbon double bond at about 5.6 and 6.1 ppm and the methyl group on double bond at about 1.9 ppm. In addition, the characteristic peaks of *N*-alkyls substituents on all MsMA monomers can be clearly observed. These results indicated that all of the MsMA monomers with high purity were successfully synthesized. Furthermore, the reaction yield of MEMA, MPMA, MBMA, and MAMA were 83%, 77%, 76%, and 80%, respectively.

### 2.2. Synthesis and Characterizations of Tri-Block Polycations PAMA-PMsMA-PEG

Due to their versatile polyelectrolyte properties and pH-responsive functions, the MsMA and its polymers are expected to serve as promising nanocarriers for gene delivery. In order to investigate the influence of the asymmetric alkyl substituents of the tertiary amine groups on siRNA delivery, five tri-block PAMA-PMsMA-PEG polycations were synthesized by multi-step sequential RAFT polymerization, as shown in **Figure 2A**. Firstly, the amino-protected P(*N*-(tert-butoxycarbonyl) aminoethyl methacrylate) (PBAMA) with pre-defined polymerization degree of about 50 was prepared

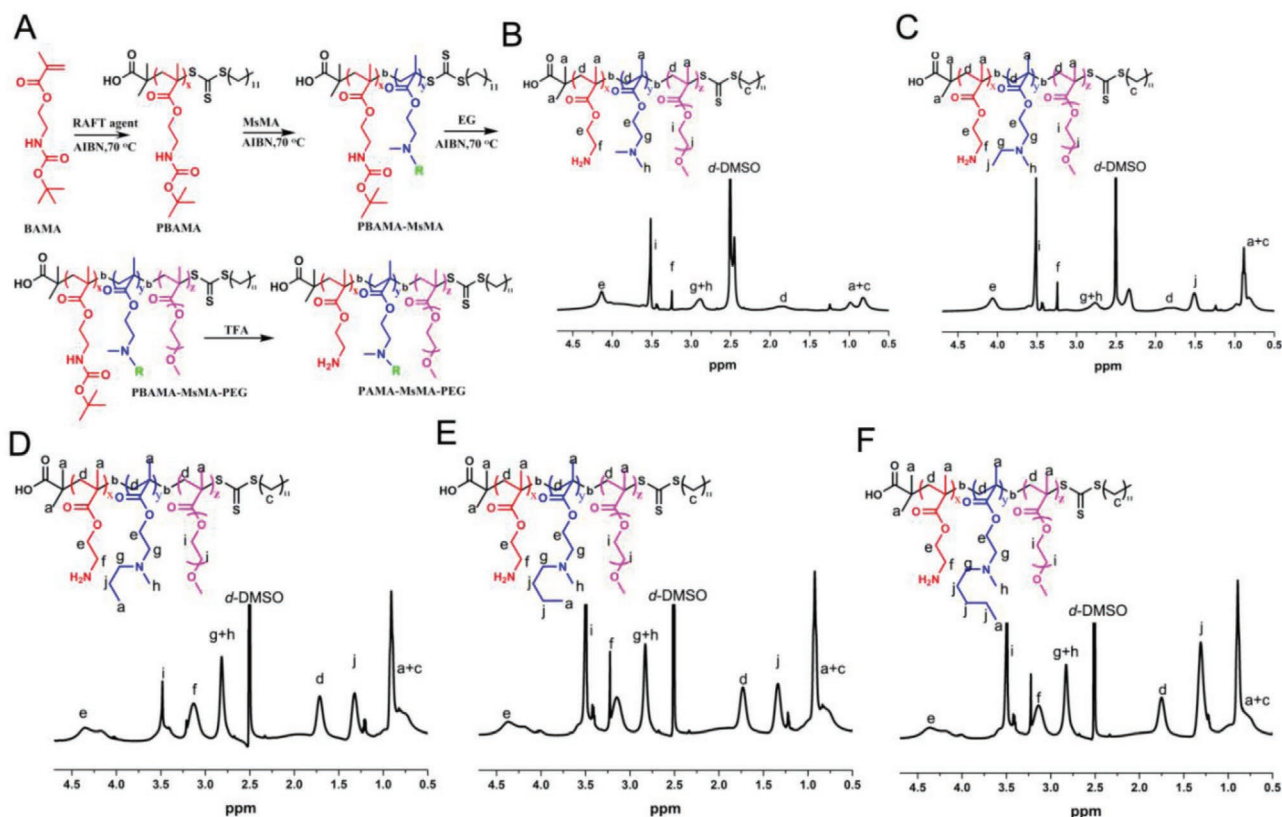


**Figure 2.** A) Synthesis routes of PAMA-PMsMA-PEG and  $^1\text{H}$  NMR of PAMA-PMsMA-PEG in *d*-DMSO (B: PAMA-PMsMA-PEG, C: PAMA-PMsMA-PEG, D: PAMA-PMPMA-PEG, E: PAMA-PMBMA-PEG, F: PAMA-PMAMA-PEG)

in the presence of S-Dodecyl-S'-( $\alpha,\alpha'$ -dimethyl- $\alpha''$ -acetic acid)-trithiocarbonate as chain transfer agent and AIBN as initiator in DMF. The PBAMA with polymerization degree of about 44 was isolated and purified by dialysis, and then was used as a macro-RAFT agent in the subsequent polymerization. And then the MsMA as pH-sensitive hydrophobic segment and polyethylene glycol methacrylate (EG) as hydrophilic segment were selected as second and third monomer, respectively, to be polymerized under similar condition to prepare the tri-block copolymers. The polymerization degree of each block was controlled by the initial molar mass ratio of monomer to RAFT agent and monomer conversion. After amino deprotection by TFA, the polycations (PAMA-PMsMA-PEG) were obtained. To confirm the chain compositions and molecular structures,  $^1\text{H}$ NMR and GPC were used to analyze

the obtained polycations. As shown in Figure 2, all  $^1\text{H}$ NMR spectra of PAMA-PMsMA-PEG show the characteristic peak (f) corresponding to the PAMA segment at about 3.2 ppm, characteristic peaks (g, h, and j) corresponding to the PMsMA segment at about 2.7 and 1.5 ppm as well as characteristic peak (i) corresponding to the PEG segment at about 3.5 ppm. All characteristic signals of PAMA, PMsMA, and PEG units could be seen clearly in the  $^1\text{H}$ NMR spectra, indicating the successful preparation of PAMA-PMsMA-PEG. In addition, all PAMA-PMsMA-PEG copolymers possess a relatively low polydispersity ( $\text{PDI} \approx 1.5$ ). The polymerization degree calculated from the ratio of  $^1\text{H}$  NMR peak area and molecular weights obtained by GPC were listed in **Table 1**. The results indicated that the triblock PAMA-PMsMA-PEG polymers with controlled chain architecture and segment composition

**Table 1.** Characterizations of PAMA-PMsMA-PEG.

Samples	AMA <sup>a</sup>	MsMA <sup>a</sup>	EG <sup>a</sup>	$M_n$ ( $\times 10^5$ Da) <sup>b</sup>	PDI <sup>b</sup>
PAMA-PMsMA-PEG	44	88	5.3	2.56	1.57
PAMA-PMsMA-PEG	44	87	5.2	2.53	1.47
PAMA-PMPMA-PEG	44	82	5.2	2.23	1.50
PAMA-PMBMA-PEG	44	90	5.4	2.68	1.49
PAMA-PMAMA-PEG	44	97	5.1	2.78	1.53

<sup>a</sup>) Polymerization degree calculated from  $^1\text{H}$  NMR; <sup>b</sup>) Determined by GPC.

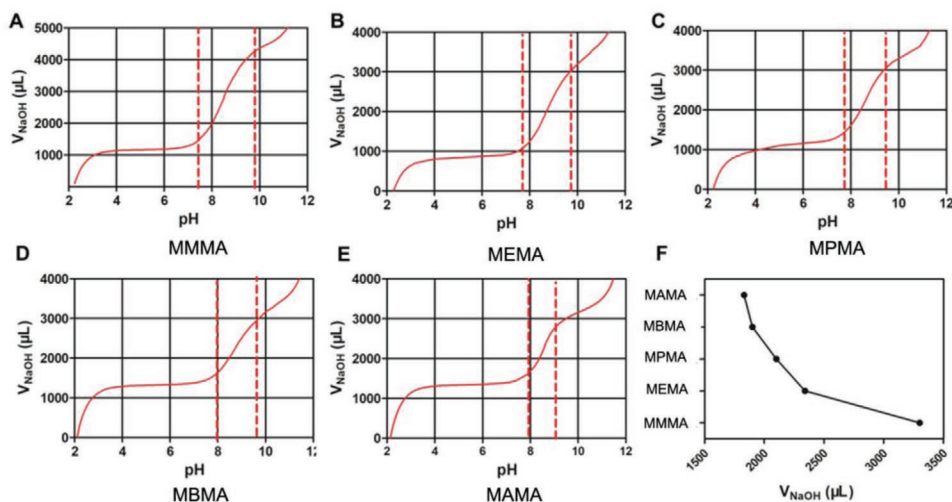


**Figure 3.** Acid-titration curves of MsMA monomers (A: MMMA, B: MEMA, C: MPMA, D: MBMA, E: MAMA) and F) consumption of NaOH solution, MsMA concentration: 2 mg mL<sup>-1</sup>, NaOH concentration: 0.1 M.

as well as predetermined molecular weight were successfully prepared by RAFT polymerization.

### 2.3. Proton Buffering Capacity of MsMA and PAMA-PMsMA-PEG

As well known, the tertiary amine-containing compounds and polymers with pK<sub>a</sub> of about 6 can undergo protonation in the acidic endosomal environment, thus resulting in an

efficient endosomal disruption and facilitating the escape from endosomes.<sup>[37,39]</sup> The new class of MsMA and PAMA-PMsMA-PEG with tunable buffering capacities were studied by acid–base titration, which was widely used to determine the buffering capacities of cationic materials and nanostructures.<sup>[38]</sup> The samples were dissolved in HCl solution and titrated by gradual addition of NaOH solution. The titration studies were conducted over a pH range of 2–12 and shown in **Figure 3A–E**. The acid–base titration results showed that, with the increase of the length of the substituted alkyl chain, the proton buffering

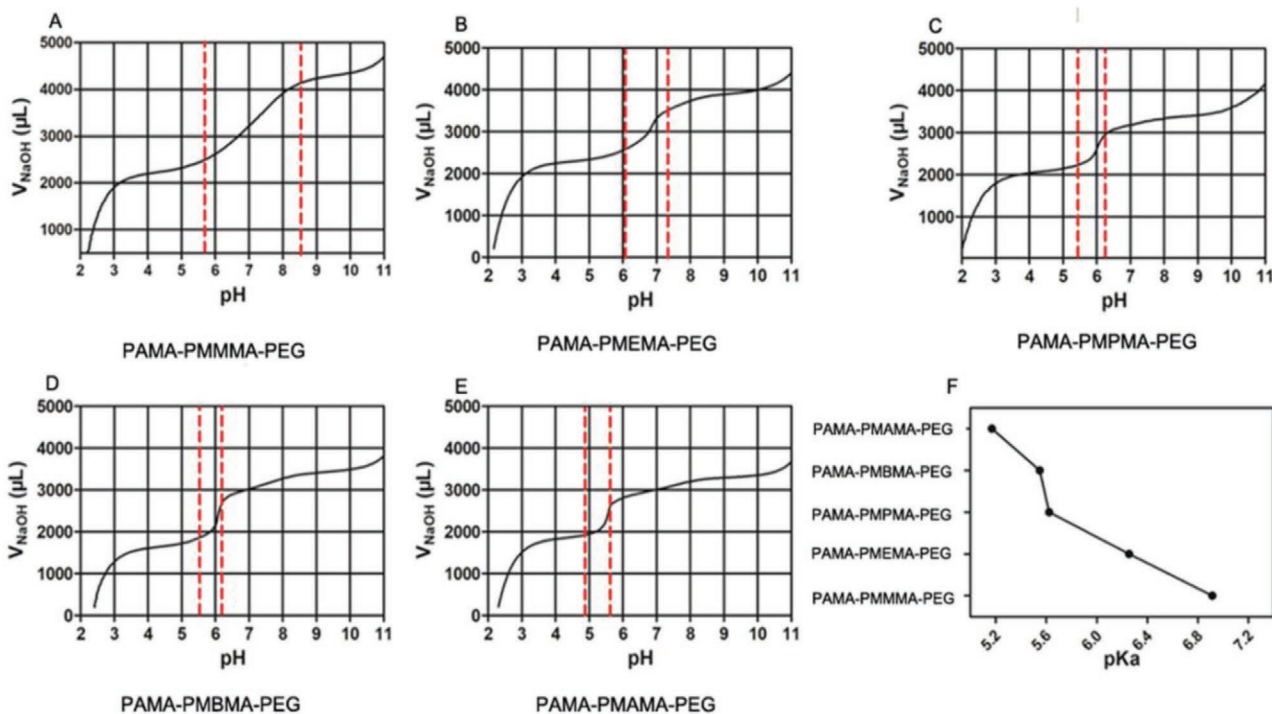


**Figure 4.** Acid-titration curves of PAMA-PMsMA-PEG polycations (A: PAMA-PMMA-PEG, B: PAMA-PEMA-PEG, C: PAMA-PMPMA-PEG, D: PAMA-PMBMA-PEG, E: PAMA-PMAMA-PEG) and F) the pK<sub>a</sub> values of PAMA-PMsMA-PEG polycations.

capacity of MsMA monomers occurred in a relatively narrower pH range. The MsMA monomers were found to require decreasing amounts of NaOH (Figure 3F) with increasing the length of the substituted alkyl chain in MsMA (carbon number from 1 to 5). It was possibly due to that longer alkyl chain could improve the steric-hindrance effect, leading to the strengthened hydrophobic interaction.

The pKa values showed important influence on siRNA delivery efficiency.<sup>[37,39]</sup> It has been reported that the pKa values of amino lipids located in 6.2–6.5 elicited efficient delivery on therapeutic agent siRNA.<sup>[39]</sup> In our previous work, we found that efficient gene knockdown was achieved by pH-sensitive polycations with pKa values of hydrophobic sections at 5.8–6.2 in vitro and in vivo.<sup>[37]</sup> Besides, we verified that pKa values affected siRNA delivery efficiency through proton sponge

effect.<sup>[40]</sup> To assess the pH-sensitive ability of the series polycations, the acid–base titration was further carried out and shown in Figure 4. The concentration of polycations was 2 mg mL<sup>-1</sup>. Based on the results in Figure 4A–E, the proton buffering capacity also mainly occurred in a narrow pH range with the same trend of MsMA monomers. The buffer capability of amine groups of MsMA. The buffer capability of cationic PAMA-PMsMA-PEG polymers as gene carriers has been proved to be favorable for the intracellular release and gene transfection. Meanwhile, it can be found from Figure 4F that the pKa values declined from 6.9 to 5.2 with increase in the length of the substituted alkyl chain, which was caused by the enhancement of interhydrophobic force of pH-sensitive section. It was worth noting that the PAMA-PMEMA-PEG possessed a pKa

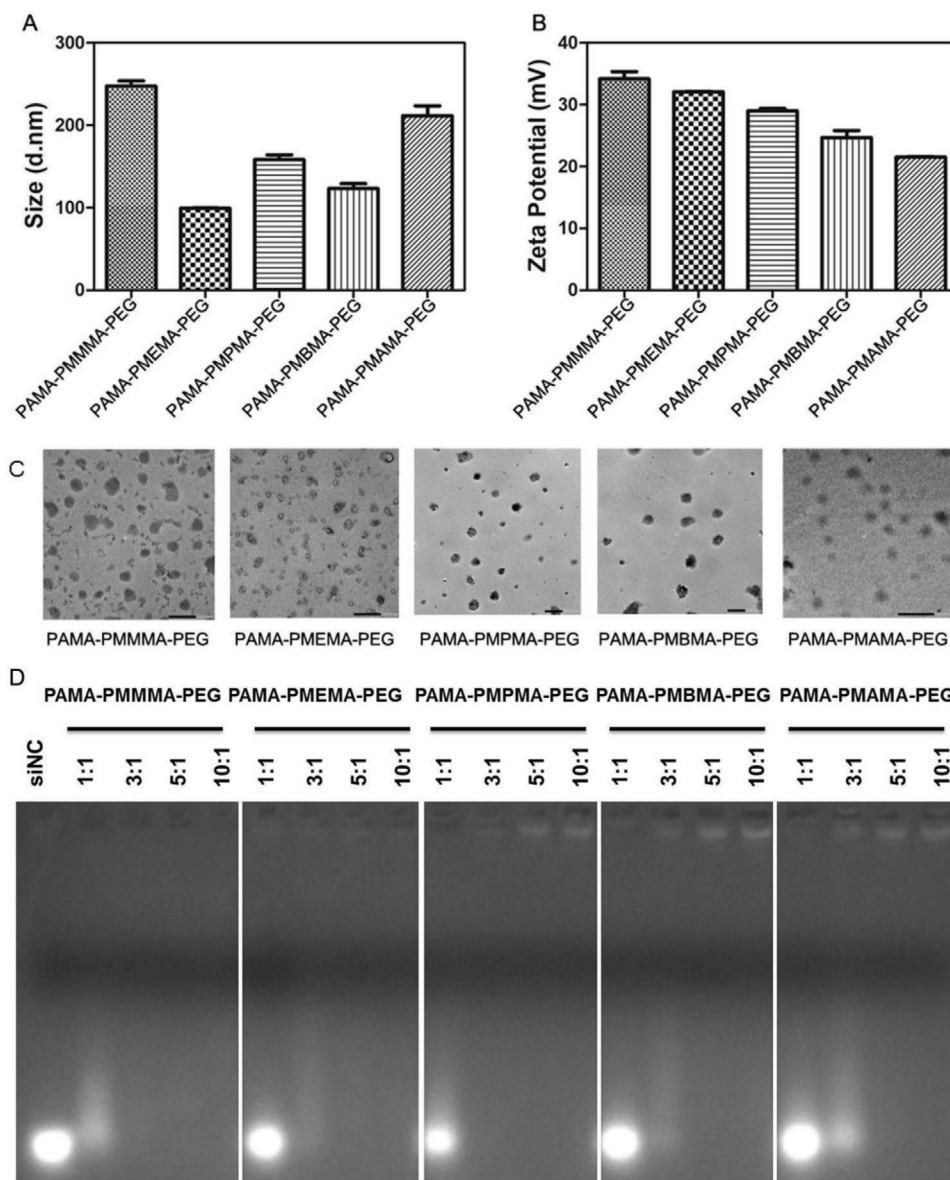


**Figure 5.** A) Sizes and B) zeta potentials and C) TEM images of PAMA-PMsMA-PEG micelles (scale bar: 200 nm). D) Gel electrophoresis analysis to determine the siRNA binding capacities of PAMA-PMsMA-PEG micelles. (siRNA: 50 nM; siNC = Negative controlled siRNA).

of 6.2, which meant that it might be very suitable for siRNA delivery. Some works reported that the pH of endosome was about 5.5–6.5.<sup>[41]</sup> Therefore, the pKa values of 6.2 indicated that PAMA-PMEMA-PEG micelles could be protonated in endosome, thus resulting in the change of osmotic pressure, which would facilitate the endosomal release of gene and thus improve the transfection efficiency of siRNA.

#### 2.4. Physicochemical Properties of PAMA-PMsMA-PEG Micelles

The obtained PAMA-PMsMA-PEG polycations were used to harvest cationic micelles. Normally, the polycations were dissolved into trifluoroethanol and dropped added into PBS or deionized water. The NPs were self-assembled through hydrophobic interaction. The sizes, zeta potentials, morphology, and distributions were determined by laser particle size analyzer and TEM. As shown in Figure 5A, the sizes of PAMA-PMMMA-PEG, PAMA-PMEMA-PEG, PAMA-PMPMA-PEG, PAMA-PMBMA-PEG, and PAMA-PMAMA-PEG micelles were about  $2477 \pm 8.7$ ,  $99.3 \pm 1.0$ ,  $123 \pm 8.8$ ,  $158.3 \pm 8.3$ , and  $211.6 \pm 11.9$  nm, respectively. And the TEM results in Figure 5C reflected all the polycations that could form micelles, and the sizes of dry particle size were smaller than that of hydrated particle size. However, the sizes of PAMA-PMsMA-PEG NPs showed no regularity with the hydrophobic sections changing. Notably, the PAMA-PMMMA-PEG and PAMA-PMAMA-PEG micelles had the biggest sizes among the five cationic micelles. For the PAMA-PMMMA-PEG, the bigger sizes might be caused by the highest pKa values, which resulted in the inattentive hydrophobic core. Nevertheless, the PAMA-PMAMA-PEG with stronger steric hindrance in the hydrophobic sections caused the bigger sizes. The zeta potentials of PAMA-PMMMA-PEG, PAMA-PMEMA-PEG, PAMA-PMPMA-PEG, PAMA-PMBMA-PEG, and PAMA-PMAMA-PEG micelles in Figure 5B were about  $34.2 \pm 1.6$ ,  $32.1 \pm 0.1$ ,  $29.0 \pm 0.5$ ,  $24.7 \pm 1.6$ , and  $21.5 \pm 0.1$  mV, respectively. It could be seen that the zeta potentials declined monotonically with increasing the length of alkyl substituent group on hydrophobic core. The nar-

rowed down proton buffering capacity of pH-sensitive sections caused the less protonation of pH-sensitive segments, further resulted in the lower zeta potentials under neutral conditions. Moreover, the considerable zeta potentials results illustrated the cationic micelles had the potential abilities of binding siRNA.

The electronegative siRNA could be bound by electropositive polycations through the charge interaction. To confirm the siRNA binding abilities of PAMA-PMsMA-PEG micelles, the gel electrophoresis analysis was implemented. As shown in Figure 5D, PAMA-PMMMA-PEG, PAMA-PMEMA-PEG, PAMA-PMPMA-PEG, and PAMA-PMBMA-PEG micelles could bind siRNA at w/w = 3/1, completely. While, PAMA-PMAMA-PEG micelles binding siRNA needed higher w/w ratio, which was up to 5/1. Lowest zeta potential of PAMA-PMAMA-PEG micelles (Figure 5B) induced its weaker siRNA binding capacity. All the results implied that the micelles formed by PAMA-PMsMA-PEG could be used for further siRNA delivery in vitro. Further, The particle sizes and zeta potentials of PEI/siRNA complexes and micelles/siRNA micelleplexes were determined by DLS. As shown in Figure S1A, Supporting Information, the sizes of PEI and micelles after binding siRNA were 90–200 nm. Moreover, the results in Figure S1B, Supporting Information, showed that the zeta potentials were  $7.5 \pm 0.72$ ,  $15.8 \pm 0.33$ ,  $11.4 \pm 0.62$ ,  $9.6 \pm 0.56$ ,  $7.7 \pm 0.60$ ,  $5.2 \pm 0.59$  mV, respectively. All the results illustrated that the micelles were suitable for in vivo siRNA delivery.

#### 2.5. Efficiencies of siRNA Transfection In Vitro

As known, an ideal siRNA delivery vehicle could not only owe high siRNA delivery efficiency but also reduce cytotoxicity. Herein, HepG2-Luc cells, which luciferase was stably expressed, were used to evaluate the gene knockdown efficiency. And the anti-firefly siRNA (siFL) was selected to silence the luciferase protein. Moreover, polyethylenimine (PEI<sub>25k</sub>) was used as positive control. As shown in Figure 6A, except for PAMA-PMBMA-PEG micelles, the level of luciferase protein decreased with the w/w ratios increasing. Excitingly,

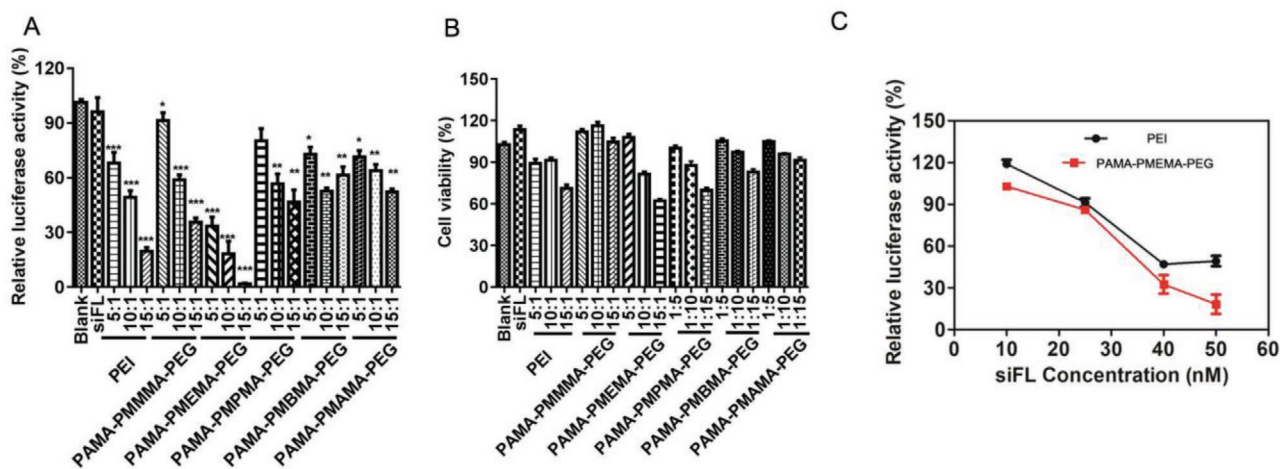


**Figure 6.** Efficiencies of gene transfection in vitro. A) Efficiency of Luciferase knockdown on HepG2-Luc cells and B) cell viability at different w/w ratios (siRNA concentration: 50 nm). C) The luciferase knockdown efficiency of PAMA-PMEMA-PEG/siFL and PEI/siFL with different siRNA concentrations on HepG2 cells (w/w = 10). Each bar represents Mean  $\pm$  SEM of three experiments. \* $p < 0.05$ , \*\* $p < 0.01$  and \*\*\* $p < 0.001$  versus Blank.

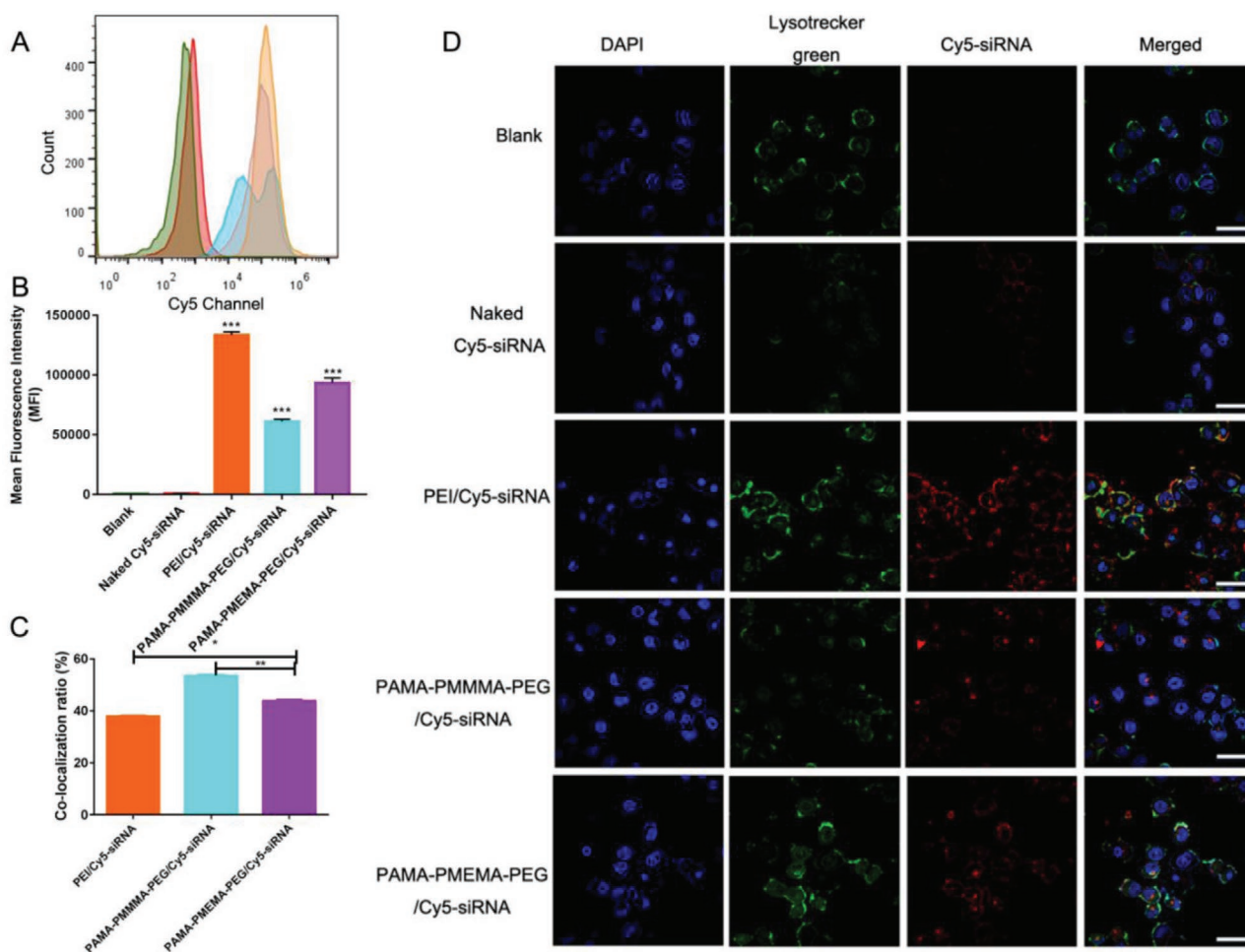


**Figure 7.** Cell uptake and endosome escape ability. A–B) Intracellular fluorescence intensities of PAMA-PMEMA-PEG NPs/Cy5-siRNA micelleplexes determined following flow cytometry at w/w = 10/1. (C) Statistics of colocalized ratios of Cy5-siRNA and LysoTracker Green. D) Intracellular distribution of Cy5-siRNA determined by CLSM. (scale bar: 50  $\mu$ m). Each bar represents Mean  $\pm$  SEM of three experiments. \* $p$  < 0.05, \*\* $p$  < 0.01 and \*\*\* $p$  < 0.001 versus Naked siRNA.

PAMA-PMEMA-PEG/siFL showed the same knockdown effect at w/w = 10/1 with PEI/siFL at w/w = 15/1. Furthermore, among the five vehicles, PAMA-PMEMA-PEG NPs showed the best gene delivery efficiency at the same w/w ratio. The luciferase protein knockdown efficiency might be related to cytotoxicity. Therefore, the cytotoxicity test was carried out. As shown in Figure 6B, there is no doubt that higher w/w ratio resulted in higher cytotoxicity. However, higher cytotoxicity (62.3%) was induced by PAMA-PMEMA-PEG/siRNA only up to w/w = 15/1. Summary, PAMA-PMEMA-PEG NPs showed efficient siRNA delivery without high cytotoxicity at w/w = 10. To further verify the effectiveness of PAMA-PMEMA-PEG micelles, we investigated the luciferase knockdown effect under different concentrations of siFL (w/w = 10). Figure 6C showed that the luciferase knockdown effect showed concentration dependence, and the gene silencing efficiency of PAMA-PMEMA-PEG/siFL was up to 81.9% with the concentrations of siFL was 50 nM. Moreover, under the same siFL concentration, PAMA-PMEMA-PEG micelles showed better luciferase protein silencing efficiency than positive control

PEI<sub>25k</sub>. Thus, it was concluded that PAMA-PMEMA-PEG micelles could deliver siRNA effectively.

## 2.6. Cell Uptake and Endosomal Escape Ability

Commonly, the internalization and escape ability are regarded as the two key factors for efficient siRNA delivery intracellular.<sup>[42]</sup> Therefore, to investigate the internalization and escape ability, the FACS and CLSM were carried out. As mentioned above, PAMA-PMEMA-PEG micelles showed the highest gene silencing efficiency among the five cationic vehicles. And PAMA-PMMA-PEG also showed somewhat siFL delivery efficiency. Therefore, the PAMA-PMMA-PEG and PAMA-PMEMA-PEG were chosen for further investigation. Cy5 labeled siRNA was used as target gene, and polyethyleneimine (PEI<sub>25k</sub>) was chosen as positive control. As shown in Figure 7A,B, compared with PAMA-PMMA-PEG/Cy5-siRNA, PAMA-PMEMA-PEG/Cy5-siRNA induced higher cell uptake efficacy. However, the cell uptake efficacies of PAMA-PMMA-PEG/Cy5-siRNA

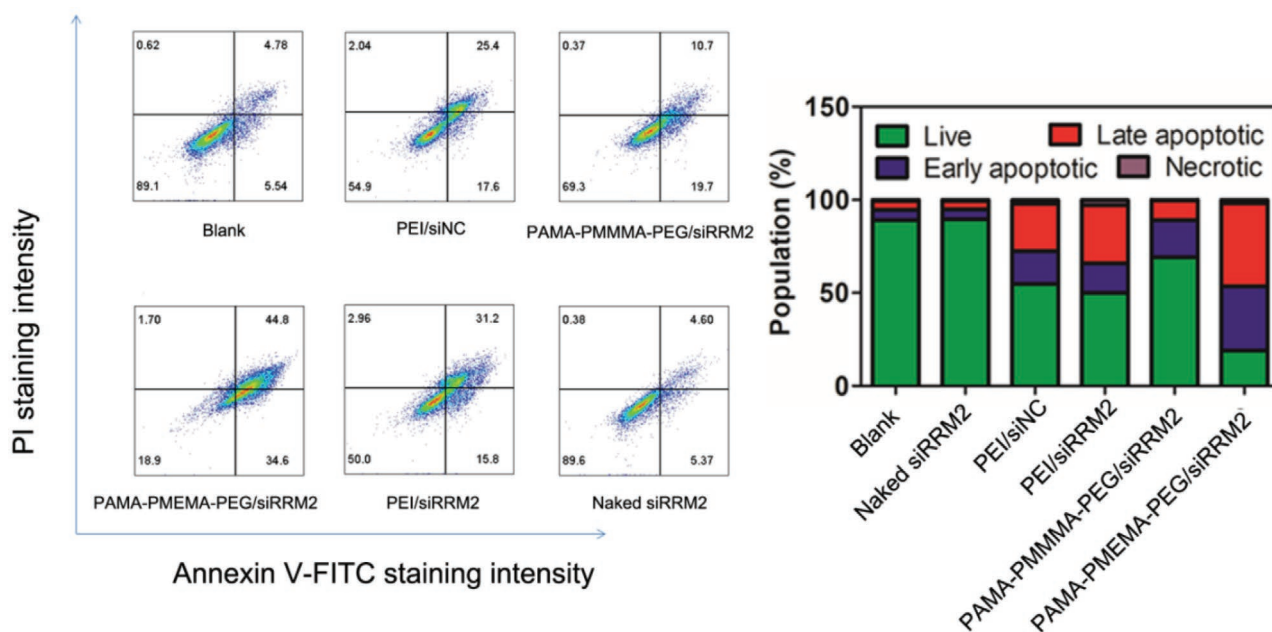


**Figure 8.** Cell apoptosis assay after treatment with siRNA-loaded PAMA-PMEMA-PEG micelles for 48 h on HepG2 cells (w/w = 10, siRNA: 50 nM).

and PAMA-PMEMA-PEG/Cy5-siRNA were lower than PEI<sub>25k</sub>/Cy5-siRNA.

Further, endosomal escape abilities of PAMA-PMMA-PEG and PAMA-PMEMA-PEG were analyzed by CLSM (Figure 7D). In Figure 7D, the signal of red represented the Cy5-siRNA escaped into the cytoplasm, whereas the yellow signal denoted the overlap of LysoTracker green and Cy5-siRNA. The co-localization ratio in Figure 7C calculated by Figure 7D showed PAMA-PMEMA-PEG owned higher escape ability than PAMA-PMMA-PEG, while, the escape ability of PEI/Cy5-siRNA was higher than PAMA-PMEMA-PEG/Cy5-siRNA. Although PAMA-PMEMA-PEG showed lower cell uptake and escape ability than PEI<sub>25k</sub>, PAMA-PMEMA-PEG displayed higher gene silencing efficiency at the same w/w ratio than PEI<sub>25k</sub>. The reason for this phenomenon was that the form of micelleplexes formed by polycationic micelles/gene could cause higher gene silencing efficiency than PICs.<sup>[16]</sup> To verify the phenomenon, Circular dichroism (CD) was carried out. As shown in Figure S2, Supporting Information, the PEI showed greater influence on the siRNA secondary structure and a red shift in the signal was observed. The results suggest a much stronger binding interaction formed with PEI, potentially distorting the siRNA and/or inhibiting proper accessibility of the payload to polymerase enzymes needed for effective transcription.

### 2.7. Anti-Tumor Cell In Vitro of PAMA-PMEMA-PEG/siRRM2 Micelleplexes

To investigate the in vitro anti-tumor efficiency of PAMA-PMEMA-PEG micelles, the apoptosis experiment was performed. PEI<sub>25k</sub> was used as the positive control, and siRRM2 was chosen as the targeted gene. Human tumors could overexpress M2 subunit of ribonucleotide reductase (RRM2), which

is related to resistance to chemotherapy,<sup>[41]</sup> malignancy,<sup>[42]</sup> DNA replication,<sup>[43]</sup> and cellular invasion.<sup>[44]</sup> Therefore the RRM2 protein knockdown by siRRM2 could suppress the tumor. After the HepG2 cells were co-cultured with PAMA-PMEMA-PEG/siRRM2 micelleplexes for 24 h, the cell apoptosis was determined. As shown in **Figure 8**, PAMA-PMEMA-PEG/siRRM2 micelleplexes resulted in the highest apoptotic and ratio of late apoptotic up to 44.8%, which was much higher than PEI/siRRM2 (31.2%). Moreover, either PAMA-PMEMA-PEG/siNC or PAMA-PMEMA-PEG/siRRM2 micelleplexes did not induce necrosis, which implied that PAMA-PMEMA-PEG/siRNA micelleplexes had good biocompatibility. Above results in vitro demonstrated that PAMA-PMEMA-PEG has great potential for further use in the design of gene vehicles. Obviously, the non-degradation induced the inherent toxicity need to be addressed. However, the asymmetric structures of tertiary amine groups introduced in gene vehicles provide multiple choices in the design of polycationic carriers for gene delivery.

### 3. Conclusion

In the presented work, a new series of asymmetric alkyl-substituted aminoethyl methacrylate were synthesized and used as pH-sensitive hydrophobic monomers to prepare a library of PAMA-PMsMA-PEG polycationic polymers as gene vehicles. Their physicochemical properties such as buffering capability, siRNA binding ability, and in vitro cytotoxicity as well as their complexation with siRNA in aqueous system were also investigated. The results indicated that the asymmetric alkyl substituents of the tertiary amine groups play a key role in the proton buffering capacity of both monomers and corresponding polycations. Increasing the length of alkyl substituent groups decreased their buffering capacity and pKa values. More

importantly, PAMA-PMEMA-PEG with pKa about 6.2 not only can exhibit high siRNA transfection efficiency and low cytotoxicity, but also can undergo protonation in the endosomal acidic environment, leading to efficient endosomal escape and considerable anti-tumor efficiency in vitro. It is expected that PAMA-PMEMA-PEG can be applied as promising carriers for efficient siRNA delivery.

#### 4. Experimental Section

**Materials:** *N*-methylethanolamine, methacryloyl chloride, 2-(dimethylamino)ethyl methacrylate (DMAEMA), azobisisobutyronitrile (AIBN), bromoethane, 1-bromopropane, 1-bromobutane, 1-bromopentane, acetonitrile (AN), dimethyl sulfoxide (DMSO), *N,N*-dimethylformamide (DMF), tetrahydrofuran (THF), triethylamine (TEA), dichloromethane (DCM), ethyl acetate (EA), petroleum ether (PE), diethyl ether, and trifluoroacetic acid (TFA) were obtained from Jiangtian Chemical Reagents Co., Ltd. (Tianjin, China). Positive control polyethylenimine 25 kDa (Gibco, USA), 2-(methylamino) ethanol, and poly(ethylene glycol methacrylate) (EG) with molecular weight of 500 were purchased from aladdin (Shanghai, China). *N*-(tert-Butoxycarbonyl) aminoethyl methacrylate (BAMA) was synthesized according to the previous study.<sup>[23]</sup>

Tris Base, Ethidium bromide, Dulbecco's modified Eagle's medium (DMEM), fetal bovine serum, trypsin, Opti-MEM, and Penicillin-streptomycin were bought from Invitrogen Corporation. Cy5-labeled siRNA (Cy5-siRNA), negative controlled siRNA (siNC), anti-firefly siRNA (siFL), and anti-RRM2 siRNA (siRRM2) were provided by Suzhou Ribo Life Science Co., Ltd. (Suzhou, Jiangsu Province, China).

**Synthesis of *N*-Methyl-*N*-Alkyl Aminoethyl Methacrylate (MsMA):** The asymmetric alkyl-substituted aminoethyl methacrylate monomers were synthesized by nucleophilic substitution and esterification reaction. Taking *N*-methyl-*N*-ethyl aminoethyl methacrylate (MEMA) as an example, *N*-methyl ethanolamine (15.022 g, 0.2 mol), 1-bromoethane (24 g, 0.22 mol), and anhydrous sodium carbonate (26.5 g, 0.25 mol) were dissolved into 400 mL acetonitrile. After the reaction at 40 °C in an oil bath for 8 h, anhydrous sodium carbonate was removed by filtration and acetonitrile was removed by rotary evaporation. The raw product was washed with saturated sodium chloride solution three times, extracted with ethyl acetate to obtain *N*-methyl-*N*-ethyl ethanolamine. And then, *N*-methyl-*N*-ethyl ethanolamine (5.3 g) and trimethylamine (7.8 g, 77 mmol) were dissolved in THF (50 mL) and cooled to 0 °C in ice-water bath. And then methacryloyl chloride was added slowly to the mixture. After reacting for 12 h, MEMA was separated by column chromatography (EA/PE = 2/5). The yield for MEMA was 80%. Other monomers were prepared by similar procedure except for the bromoalkyl. All the monomers were characterized by <sup>1</sup>H NMR and stored for further usage. The siRNA sequences were listed in Table S1, Supporting Information.

**Synthesis and Characterizations of PAMA-PMsMA-PEG:** The tri-block PAMA-PMsMA-PEG polymers were synthesized by a tri-step sequential RAFT polymerization. The first block amino-protected poly[*N*-(tert-butoxycarbonyl) aminoethyl methacrylate](PBAMA) with pre-ordained polymerization degree of about 50 was prepared in the presence of *S*-Dodecyl-*S'*-( $\alpha,\alpha'$ -dimethyl- $\alpha'$ -acetic acid)-trithiocarbonate as RAFT agent and AIBN as initiator in DMF. Typically, RAFT agent (95.6 mg 0.26 mmol), *N*-(tert-butoxycarbonyl) aminoethyl methacrylate (3 g, 13.1 mmol) and initiator AIBN (3.28 mg, 0.02 mmol) were dissolved in DMF (5 mL). After complete dissolution and three freeze-pump-thaw cycles, the flask was placed in a thermostatic water bath at 70 °C for about 24 h under Argon atmosphere. The PBAMA was isolated and purified by dialysis and lyophilization, and then was used as a macro-RAFT agent in the subsequent polymerization to prepare PBAMA-PMsMA with pre-ordained polymerization degree of about 100 and PBAMA-*b*-PMsMA-PEG. After deprotection by TFA, the polycations PAMA-PMsMA-PEG were obtained. Taking PAMA-PMEMA-PEG as an example, PBAMA (0.51 g, 0.05 mmol), MEMA (0.85 g, 5 mmol),

and AIBN (1.57 mg, 0.01 mmol) were dissolved in DMF (3 mL). The pretreatment, polymerization, and post-treatment were same as the procedure mentioned above. And then the obtained PBAMA-PMEMA was used as macro-RAFT agent to polymerize with poly(ethylene glycol methacrylate) at molar ratio of 1:4 to obtain PBAMA-PMEMA-PEG under same condition. Finally, The PAMA-PMEMA-PEG was obtained by deprotection by TFA. Other PAMA-PMsMA-PEG polymers were synthesized by same procedure except for the MsMA. All the polycations were stored and characterized by <sup>1</sup>H NMR and GPC for further usage.

The molecular weights and polydispersity index (PDI) of the polymers were measured with a Waters 1515 gel permeation chromatographer (GPC, Waters company, Milford, USA) equipped with refractive index detector, using polystyrene as the standard material for calibration and DMF as the eluent at a flow rate of 1 mL min<sup>-1</sup>. <sup>1</sup>H NMR spectra of MsMA and PAMA-PMsMA-PEG were recorded on a Varian Inova-500M instrument (Varian Inc., Palo Alto, USA) with CDCl<sub>3</sub> or *d*-DMSO as a solvent and tetramethylsilane (TMS) as the internal standard.

**Preparation of PAMA-PMsMA-PEG Micelles:** Typically, 10 mg PAMA-PMsMA-PEG was dissolved in 1 mL trifluoroethanol and drop added into deionized water (10 mL). Waiting for the trifluoroethanol to evaporate, the nanoparticles concentration was adjusted to 1 mg mL<sup>-1</sup> for further usage. The zeta potentials and sizes of PAMA-PMsMA-PEG nanoparticles and micelles/siRNA micelleplexes were determined by dynamic light scattering (Zetasizer Nano ZS, Malvern, UK).

**Determination of siRNA Binding Capacities:** Agarose gel retardation assay was used to determine the siRNA binding capacity. PAMA-PMsMA-PEG nanoparticles and siRNA (50 nM) with w/w ratios of 1/1, 3/1, 5/1, and 10/1 were incubated at room temperature for 20 min, and mixed with 3  $\mu$ L 6 $\times$  loading buffer. And then, the volume was adjusted to 20  $\mu$ L. Finally, the solution was added into agarose gel hole (2%), which contained ethidium bromide (5  $\mu$ L). The electrophoresis was carried out under 120 V for 20 min in 1 $\times$  TAE running buffer. Finally, the gel was characterized at UV light (254 nm, VDS thermal imaging system).

**Acid-Base Titrations of MsMA and Tri-Block Polycations:** The pH-sensitive abilities of MsMA and tri-block polycations were carried out by acid-base titrations. In a word, 40 mg materials dissolved in 0.1 M HCl (3 mL). After that, the volume was adjusted to 20 mL. And then, NaOH solution (0.1 M) was drop added. The pH values and NaOH consumption volumes were recorded respectively.

**Luciferase Assay:** HepG2-Luc cells, which expressed luciferase protein stably, were plated in 24-well plates for 24 h. Then the medium changed with Opti-MEM (0.5 mL), the PAMA-PMsMA-PEG/siFL (siRNA: 50 nM) micelleplexes with different w/w ratios were added, respectively. After transfecting for 4 h, the medium was replaced with DMEM (1 mL) and cultured for another 20 h. After that, HepG2-Luc cells were washed with PBS and lysed with passive lysis buffer (100  $\mu$ L) and made sure the cells lysis completely. Finally, centrifuged for 1 min at 12 000 rpm, and collected the supernatant for luminescence measurements by Multi-Mode Microplate Reader (Synergy HT, BioTek, USA).

**Cell Viability:** HepG2 cells were incubated in 96-well for 24 h. Cells were treated with PAMA-PMsMA-PEG/siRNA micelleplexes for 24 h. Then, cells were washed with PBS three times and the medium was replaced with fresh DMEM medium containing 10  $\mu$ L CCK-8. After 20 min, the absorbance of medium was determined by Multi-Mode Microplate Reader.

**Confocal Laser Scanning Observation:** The intracellular distribution of PAMA-PMsMA-PEG/Cy5-siRNA complexes was determined by laser scanning confocal microscope. In summary, HepG2 cells were plated into 35 mm dishes for 24 h. And cells were treated with PAMA-PMsMA-PEG/Cy5-siRNA micelleplexes for 4 h. And then, cells were washed with PBS three times and stained with LysoTracker Green (staining endosomes and lysosome) and DPAI (staining nuclei). At last, Zeiss confocal microscope (LSM700, Carl Zeiss, Germany) was used to image cells.

**Flow Cytometry Detection:** HepG2 cells (1  $\times$  10<sup>5</sup>) were seeded into 6-well plate, and cultured for 24 h. Then the medium was replaced with Opti-MEM, and the PEI/Cy5-siRNA and PAMA-PMsMA-PEG/Cy5-siRNA complexes (w/w = 10/1) were added to culture 4 h. Finally, the tumor

cells were digested and washed three times with PBS. Fast test was administrated under FACS Caliber flow cytometry (Becton Dickinson, San Jose, CA, USA).

**Apoptosis Analysis:** HepG2 cells ( $1 \times 10^5$ ) were incubated in 6-well plate for 24 h. Further, the cells were treated with PBS, siRRM2, PEI/siNC, PEI/siRRM2, PAMA-PMEMA-PEG/siNC, and PAMA-PMEMA-PEG/siRRM2 for 24 h (w/w = 10/1, siRNA: 50 nM). The cells were digested and washed with PBS three times, as well as stained with PI and Annexin V-FITC. Fast characterization was carried out under FACS Caliber flow cytometry (Becton Dickinson, San Jose, CA, USA).

**Statistical Analysis:** Graph Pad Prism 5.0 software was used to analyze the data. Results were presented as mean  $\pm$  SEM. For statistical comparison, student's *t*-test and one way-ANOVA were used and  $P < 0.05$  was considered statistically significant.

## Supporting Information

Supporting Information is available from the Wiley Online Library or from the author.

## Acknowledgements

This work was supported by the National Natural Science Foundation of China (No. 31671021, 51703246) and Natural Science Foundation of Tianjin City (19JCYBJC17200), CAMS Innovation Fund for Medical Sciences (CIFMS, 2016-12M-3-022).

## Conflict of Interest

The authors declare no conflict of interest.

## Data Availability Statement

Research data are not shared.

## Keywords

asymmetric structure, pH-sensitive polycations, proton buffering capacity, siRNA delivery

Revised: March 7, 2021  
Published online: March 26, 2021

- [1] S. M. Elbashir, J. Harborth, W. Lendeckel, A. Yalcin, K. Weber, T. Tuschl, *Nature* **2001**, *411*, 494.
- [2] K. V. Morris, S. W. L. Chan, S. E. Jacobsen, D. J. Looney, *Science* **2004**, *305*, 1289.
- [3] D. Bumcrot, M. Manoharan, V. Koteliansky, D. W. Y. Sah, *Nat. Chem. Biol.* **2006**, *2*, 711.
- [4] H. Yin, R. L. Kanasty, A. A. Eltoukhy, A. J. Vegas, J. R. Dorkin, D. G. Anderson, *Nat. Rev. Genet.* **2014**, *15*, 541.
- [5] W. J. Huang, X. X. Wang, C. R. Wang, L. L. Du, J. H. Zhang, L. D. Deng, H. Q. Cao, A. J. Dong, *J. Mater. Chem. B* **2019**, *7*, 965.
- [6] S. C. Semple, A. Akinc, J. X. Chen, A. P. Sandhu, B. L. Mui, C. K. Cho, D. W. Y. Sah, D. Stebbing, E. J. Crosley, E. Yaworski, I. M. Hafez, J. R. Dorkin, J. Qin, K. Lam, K. G. Rajeev, K. F. Wong, L. B. Jeffs, L. Nechev, M. L. Eisenhardt, M. Jayaraman, M. Kazem, M. A. Maier, M. Srinivasulu, M. J. Weinstein, Q. M. Chen, R. Alvarez, S. A. Barros, S. De, S. K. Klimuk, T. Borland, V. Kosovrasti, W. L. Cantley, Y. K. Tam, M. Manoharan, M. A. Ciufolini, M. A. Tracy, A. de Fougere lles, I. MacLachlan, P. R. Cullis, T. D. Madden, M. J. Hope, *Nat. Biotechnol.* **2010**, *28*, 172.
- [7] J. Kaiser, *Science* **2020**, *367*, 131.
- [8] D. Schaffert, E. Wagner, *Gene Ther.* **2008**, *15*, 1131.
- [9] W. J. Sun, W. Y. Ji, J. M. Hall, Q. Y. Hu, C. Wang, C. L. Beisel, Z. Gu, *Angew. Chem., Int. Ed.* **2015**, *54*, 12029.
- [10] A. Mokhtarzadeh, A. Alibakhshi, H. Yaghoobi, M. Hashemi, M. Hejazi, M. Ramezani, *Expert Opin. Biol. Ther.* **2016**, *16*, 771.
- [11] X. Y. Bai, M. Kong, X. J. Wu, C. Feng, H. J. Park, X. G. Chen, *J. Mater. Chem. B* **2018**, *6*, 5910.
- [12] E. Mastrobattista, W. E. Hennink, *Nat. Mater.* **2012**, *11*, 10.
- [13] M. E. Davis, J. E. Zuckerman, C. H. J. Choi, D. Seligson, A. Tolcher, C. A. Alabi, Y. Yen, J. D. Heidel, A. Ribas, *Nature* **2010**, *464*, 1067.
- [14] K. L. Kozielski, S. Y. Tzeng, B. A. H. De Mendoza, J. J. Green, *ACS Nano* **2014**, *8*, 3232.
- [15] J. H. Zhou, Y. D. Wu, C. R. Wang, Q. Cheng, S. C. Han, X. X. Wang, J. H. Zhang, L. D. Deng, D. Y. Zhao, L. L. Du, H. Q. Cao, Z. C. Liang, Y. Y. Huang, A. J. Dong, *Nano Lett.* **2016**, *16*, 6916.
- [16] Z. Tan, Y. Jiang, W. Zhang, L. Karls, T. P. Lodge, T. M. Reineke, *J. Am. Chem. Soc.* **2019**, *141*, 15804.
- [17] D. C. Zhu, H. J. Yan, Z. X. Zhou, J. B. Tang, X. R. Liu, R. Hartmann, W. J. Parak, N. Feliu, Y. Q. Shen, *Biomater. Sci.* **2018**, *6*, 1800.
- [18] A. Kano, K. Moriyama, T. Yamano, I. Nakamura, N. Shimada, A. Maruyama, *J. Controlled Release* **2011**, *149*, 2.
- [19] M. Byrne, D. Victory, A. Hibbitts, M. Lanigan, A. Heise, S. A. Cryan, *Biomater. Sci.* **2013**, *1*, 1223.
- [20] T. Z. Yu, X. X. Liu, A. L. Bolcato-Bellemin, Y. Wang, C. Liu, P. Erbacher, F. Q. Qu, P. Rocchi, J. P. Behr, L. Peng, *Angew. Chem., Int. Ed.* **2012**, *51*, 8478.
- [21] X. D. Xu, J. Wu, Y. L. Liu, P. E. Saw, W. Tao, M. Yu, H. Zope, M. Si, A. Victorious, J. Rasmussen, D. Ayyash, O. C. Farokhzad, J. J. Shi, *ACS Nano* **2017**, *11*, 2618.
- [22] X. D. Xu, J. Wu, Y. L. Liu, M. Y. Yu, L. L. Zhao, X. Zhu, S. Bhasin, Q. Li, E. Ha, J. J. Shi, O. C. Farokhzad, *Angew. Chem., Int. Ed.* **2016**, *55*, 7091.
- [23] C. R. Wang, L. L. Du, J. H. Zhou, L. W. Meng, Q. Cheng, C. Wang, X. X. Wang, D. Y. Zhao, Y. Y. Huang, S. Q. Zheng, H. Q. Cao, J. H. Zhang, L. D. Deng, Z. C. Liang, A. J. Dong, *ACS Appl. Mater. Interfaces* **2017**, *9*, 32463.
- [24] S. D. Li, L. Huang, *J. Controlled Release* **2010**, *145*, 178.
- [25] C. Y. Sun, S. Shen, C. F. Xu, H. J. Li, Y. Liu, Z. T. Cao, X. Z. Yang, J. X. Xia, J. Wang, *J. Am. Chem. Soc.* **2015**, *137*, 15217.
- [26] H. J. Kim, T. Ishii, M. Zheng, S. Watanabe, K. Toh, Y. Matsumoto, N. Nishiyama, K. Miyata, K. Kataoka, *Drug Delivery Transl. Res.* **2014**, *4*, 50.
- [27] H. J. Kim, K. Miyata, T. Nomoto, M. Zheng, A. Kim, X. Liu, H. Cabral, R. J. Christie, N. Nishiyama, K. Kataoka, *Biomaterials* **2014**, *35*, 4548.
- [28] T. Qi, B. L. Chen, Z. H. Wang, H. L. Du, D. C. Liu, Q. Q. Yin, B. Y. Liu, Q. Zhang, Y. G. Wang, *Biomaterials* **2019**, *213*, 119219.
- [29] M. Wojnilowicz, A. Glab, A. Bertucci, F. Caruso, F. Cavalieri, *ACS Nano* **2019**, *13*, 187.
- [30] K. Miyata, N. Nishiyama, K. Kataoka, *Chem. Soc. Rev.* **2012**, *41*, 2562.
- [31] S. Roy, D. Zhu, W. J. Parak, N. Feliu, *ACS Nano* **2020**, *14*, 8012.
- [32] H. J. Yan, D. C. Zhu, Z. X. Zhou, X. Liu, Y. Piao, Z. Zhang, X. R. Liu, J. B. Tang, Y. Q. Shen, *Biomaterials* **2018**, *178*, 559.
- [33] Z. X. Zhou, X. R. Liu, D. C. Zhu, Y. Wang, Z. Zhang, X. F. Zhou, N. S. Qiu, X. S. Chen, Y. Q. Shen, *Adv. Drug Delivery Rev.* **2017**, *115*, 115.
- [34] J. Q. Wang, W. W. Mao, L. L. Lock, J. B. Tang, M. H. Sui, W. L. Sun, H. G. Cui, D. Xu, Y. Q. Shen, *ACS Nano* **2015**, *9*, 7195.
- [35] A. Wittrup, A. Ai, X. Liu, P. Hamar, R. Trifonova, K. Charisse, M. Manoharan, T. Kirchhausen, J. Lieberman, *Nat. Biotechnol.* **2015**, *33*, 870.



- [36] J. Gilleron, W. Querbes, A. Zeigerer, A. Borodovsky, G. Marsico, U. Schubert, K. Manygoats, S. Seifert, C. Andree, M. Stoter, H. Epstein-Barash, L. G. Zhang, V. Koteliansky, K. Fitzgerald, E. Fava, M. Bickle, Y. Kalaidzidis, A. Akinc, M. Maier, M. Zerial, *Nat. Biotechnol.* **2013**, *31*, 638.
- [37] L. L. Du, C. R. Wang, L. W. Meng, Q. Cheng, J. H. Zhou, X. X. Wang, D. Y. Zhao, J. H. Zhang, L. D. Deng, Z. C. Liang, A. J. Dong, H. Q. Cao, *Biomaterials* **2018**, *176*, 84.
- [38] Y. Li, Z. H. Wang, Q. Wei, M. Luo, G. Huang, B. D. Sumer, J. M. Gao, *Polym. Chem.* **2016**, *7*, 5949.
- [39] M. Jayaraman, S. M. Ansell, B. L. Mui, Y. K. Tam, J. X. Chen, X. Y. Du, D. Butler, L. Eltepu, S. Matsuda, J. K. Narayanannair, K. G. Rajeev, I. M. Hafez, A. Akinc, M. A. Maier, M. A. Tracy, P. R. Cullis, T. D. Madden, M. Manoharan, M. J. Hope, *Angew. Chem., Int. Ed.* **2012**, *51*, 8529.
- [40] C. Wang, X. Wang, L. Du, Y. Dong, A. Dong, *ACS Appl. Mater. Interfaces* **2021**, *13*, 2218.
- [41] M. S. Duxbury, H. Ito, M. J. Zinner, S. W. Ashley, E. E. Whang, *Oncogene* **2004**, *23*, 1539.
- [42] X. Liu, B. Zhou, L. Xue, J. Shih, K. Tye, W. Lin, C. Qi, P. Chu, F. Un, W. Wen, Y. Yen, *Clin. Cancer Res.* **2006**, *12*, 6337.
- [43] J. D. Heidel, J. Y. C. Liu, Y. Yen, B. S. Zhou, B. S. E. Heale, J. J. Rossi, D. W. Bartlett, M. E. Davis, *Clin. Cancer Res.* **2007**, *13*, 2207.
- [44] H. Ito, M. Duxbury, M. J. Zinner, S. W. Ashley, E. E. Whang, *Surgery* **2004**, *136*, 548.